



J. Serb. Chem. Soc. 87 (6) 749–760 (2022)
JSCS–5555

Influence of boron doping on characteristics of glucose-based hydrothermal carbons

ANA M. KALIJADIS¹, MARINA M. MALETIĆ^{2*#}, ANĐELIKA Z. BJELAJAC^{2,3},
BILJANA M. BABIĆ⁴, TAMARA Z. MINOVIĆ ARSIĆ¹ and MARIJA M. VUKČEVIĆ^{5#}

¹Department of Materials „Vinča” Institute of Nuclear Sciences – National Institute of the Republic of Serbia, University of Belgrade, Mike Petrovića Alasa 12–14, 11000 Belgrade, Serbia, ²Innovation Center of the Faculty of Technology and Metallurgy, Karnegijeva 4, 11000 Belgrade, Serbia, ³C2N – Centre for Nanoscience and NanoTechnology, University Paris-Saclay, 10 boulevard Thomas Gobert, 91120 Palaiseau, France, ⁴Institute of Physics – National Institute of the Republic of Serbia, University of Belgrade, Pregrevica 118, 11080 Belgrade, Serbia and ⁵Faculty of Technology and Metallurgy, University of Belgrade, Karnegijeva 4, 11000 Belgrade, Serbia

(Received 11 October 2021, revised 30 December 2021, accepted 3 January 2022)

Abstract: In this study, the influence of boron doping on structural and surface properties of carbon material synthesized by a hydrothermal method was investigated, and the obtained results were compared with the previously published influence that boron has on characteristics of carbonized boron-doped hydrothermal carbons (CHTCB). Hydrothermal carbons doped with boron (HTCB) were obtained by the hydrothermal synthesis of glucose solutions with different nominal concentrations of boric acid. It was found that glucose based hydrothermal carbon does not have developed porosity, and the presence of boron in their structure has insignificant influence on it. On the contrary, additional carbonization increases the specific surface area of the undoped sample, while an increase in boron content drastically decreases the specific surface area. Boron doping leads to a decrease in the amount of surface oxygen groups, for both, hydrothermally synthesized and additionally carbonized materials. Raman analysis showed that the boron content does not affect a structural arrangement of the HTCB samples, and Raman structural parameters show a higher degree of disorder, compared to the CHTCB samples. Comparison of structural and surface characteristics of hydrothermal carbons and carbonized materials contributes to the study of the so far, insufficiently clarified influence that boron incorporation has on the material characteristics.

Keywords: hydrothermal synthesis; boric acid; Raman analysis; specific surface area; surface oxygen groups.

* Corresponding author. E-mail: mvukasinovic@tmf.bg.ac.rs

Serbian Chemical Society member.

<https://doi.org/10.2298/JSC211011001K>

INTRODUCTION

Carbon can be found in a wide variety of allotropes from crystalline (diamond, graphite) to amorphous (carbon black, activated carbon, glassy carbon, *etc.*). In the past decades, nanostructured forms of crystalline carbon have received increasing attention due to their remarkable properties based on their unusual physicochemical properties.^{1,2} The main disadvantage of using such crystalline nanocarbons for energy and environmental-related application is their high production costs. This is related to the rather expensive precursors and catalysts utilized, as well as to the complicated apparatus needed for their production normally involving high temperatures.

Conversely, hydrothermal carbonization has gained increasing attention in the field of material science, since it can successfully exploit cheap and renewable biomass as the carbon precursor.^{3–6} In addition, hydrothermal carbonization demonstrates the capability of producing highly functionalized carbon material under a mild temperature (≈ 200 °C) and self-generated pressure.^{7,8} The resultant materials were solid hydrophilic carbon microspheres with abundant functional groups on the surface. The characteristics of these microspheres, such as size, microstructure, and crystallinity, are controllable by the synthesis process and its respective experimental parameters.⁹ It was reported that the sizes of the carbon spheres from styrene as a precursor can be controlled quite well by adjusting the pyrolysis parameters.¹⁰ The carbon spheres obtained after pyrolysis showed a higher carbonization degree than those obtained by hydrothermal carbonization because the pyrolysis occurs at much higher temperatures.

However, just because of its low process temperature, the materials obtained by hydrothermal carbonization have some limiting factors, such as low ash content, low porosity, low aromatic structure, and low recalcitrance,⁸ and the possibility to modify some of these properties is crucial for the expansion of its application. One of the most important prerequisites for the successful performance of hydrothermal carbonization-based materials in various applications is material functionality. Typical materials produced by hydrothermal carbonization contain polar surface oxygen groups, such as $-\text{COOH}$, $-\text{OH}$ and $-\text{C}=\text{O}$.¹¹ The flexibility of hydrothermal carbonized materials is that groups present on the surface can be further functionalized. Two of the most commonly used methods of functionalization are: *in situ* functionalization and post-modification strategies. Heteroatom doping represents one of the possibilities for obtaining functionalized material *in situ* in one-step (bulk/surface) functionalization.^{12,13} Among many heteroatoms, boron has been proved to induce interesting electronic properties to carbon materials.^{14–17} Boron with its electrical structure shows a tendency for substitution incorporation in carbon structure up to its solid solubility limit. Above this limit, boron atoms have been shown to occupy interstitial positions in the lattice and have a disturbing effect on the structural properties.¹⁸ The

presence of substitutionally bonded boron atoms in a carbon structure inhibit the C–O₂ reaction because boron acts as an electron acceptor, which could decrease the electron density at the carbon crystallite edges and this consequently leads to a reduction of both the number of active sites and the reactivity of these sites.¹⁹ Nevertheless, a previous study showed that the number and nature of active sites and, consequently, the formation of surface oxides are dependent on the distribution of boron in the precursors.^{20,21}

High-temperature treatment (HTT) of hydrothermally derived spheres represents one of the post-modification strategies that could lead to the removal of most of the oxygenated groups and convert the structure into a turbostratic-like disordered carbon structure with aromatic character and hydrophobic properties.¹² A previous study was focused on the characterization of boron-doped hydrothermal carbon with post high temperature treatment.²² It was shown that the synergy of boron doping and thermal treatment to 1000 °C facilitated the preparation of a material with specific structural and surface chemistry characteristics, which are crucial for the application of the obtained material as a carbon paste electrode.

Many previous studies were focused on both applications and fundamental aspects motivated by the interest in producing carbonaceous powders with tunable sizes and surface properties.^{23–26} To the best of our knowledge, there is no publication regarding the characterization of boron-doped hydrothermal carbons. Moreover, the influence that boron atoms have on the characteristics of carbon materials have not yet been fully clarified and, based on previous work,^{20–22} it could be quite different, depending on boron concentration and distribution in the carbon material, the type of the carbon material and the stage of its modification. Considering these facts, the present study was aimed at the clarification of the influence of boron doping on the structural and surface properties of carbons synthesized by hydrothermal carbonization and the comparison of the obtained results with previously published results that are related to carbonized glucose based hydrothermal carbons. This comparison could provide a better insight into the influence of B doping on the structural and surface characteristics of carbon materials in the different stages of synthesis.

EXPERIMENTAL

To produce boron doped hydrothermal carbon (HTCB) samples, a 2 M aqueous solution of D(+)-glucose was prepared. Boric acid was used as the source of boron and it was added to the starting solution to obtain nominal boron concentrations of 0.0 (undoped sample), 0.2, 0.6 and 1.0 wt. %. After sealing, the autoclave was heated in a programmable oven for 24 h at 180 °C. The obtained samples were filtered, washed with distilled water and ethanol, and marked as hydrothermally carbonized samples: HTCB₀, HTCB_{0.2}, HTCB_{0.6} and HTCB₁.

In order to reveal the influence of boron doping on the surface and structural characteristics of the hydrothermally synthesized carbons, the HTCB samples were characterized and the obtained results compared with the previously published²² characteristics of boron-doped

hydrothermal carbons, synthesized in the same way, subsequently carbonized in nitrogen to 1237 K, and marked as CHTCB₀, CHTCB_{0.2}, CHTCB_{0.6} and CHTCB₁.

Final boron concentrations were determined using inductively coupled plasma mass spectrometry (ICP-MS, Agilent 7500ce) with a detection limit for B of 0.1 g dm⁻³. The samples were prepared according to the preparation method described in the literature: the samples were digested by fusing with sodium carbonate and dissolving the resulting melt in water with a small amount of hydrochloric acid.¹⁴

Raman spectra were taken with an Advantage 532 Raman spectrometer (DeltaNu Inc.) by a frequency doubled diode pumped YAG type laser operating at 532 nm.

Surface structure and morphology were studied by scanning electron microscopy (Mira Tescan X3).

Qualitative analyses of surface oxygen groups of samples were performed by Fourier transform infrared spectroscopy (FT-IR, Bomem MB-Series, Hartmann & Braun). The FT-IR measurements were performed at wavelengths in the range 4000 to 400 cm⁻¹.

The specific surface area of the HTCB samples was analyzed using the Surfer (Thermo Fisher Scientific, USA), and the mesopore surface and micropore volume were estimated using the *t*-plot method.²⁷ The tested samples were degassed at 100 °C for 4 h, and N₂ adsorption and desorption isotherms were obtained at the temperature of liquid nitrogen.

The Boehm method²⁸ was used for the determination of acidic and basic oxygen groups, present on the surface of the HTCB and CHTCB samples. For determination of the acidic sites, small quantities (0.1 g) of HTCB and CHTCB samples were mixed with 10 cm³ of base solutions (0.1 M NaOH, 0.1 M NaHCO₃ or 0.05 M Na₂CO₃) in 25 cm³ beakers. The beakers were sealed and shaken for 24 h. The solutions were then filtered and titrated with 0.05 M H₂SO₄. Similarly, the basic sites were determined by mixing 0.1 g of the examined materials with 10 cm³ of 0.1 M HCl. The obtained solutions were titrated with 0.1 M NaOH.

RESULTS AND DISCUSSION

The presence of B in the structure of the examined samples was confirmed by ICP-MS, and the results are given in Table I. Considering that for the B-doped samples the initial concentrations of boron in the starting glucose solution were 0.2, 0.6 and 1.0 wt. %, it could be concluded that a considerable portion (60–72 %) of the boron atoms was incorporated into the HTCB samples. In contrast to that, the boron content in carbonized samples was significantly reduced and ranged from 0.09 to 0.19 wt.%,²² indicating that a significant amount of boron is lost during thermal treatment. The results show that the content of dopant in the carbon materials obtained by the subsequent carbonization is not proportional to the concentration of dopant in the precursor. Furthermore, these results indicate that the chemical bonds between the boron and carbon atoms within the HTCB samples are quite weak, especially for the samples with the high nominal concentration of boron (0.6 and 1.0 wt. %), since most of the boron atoms leave the material during HTT, and only a small portion of the boron atoms manage to create chemical bonds and incorporate into the the structure of the carbonized material.

The SEM photographs of HTCB samples are shown in Fig. 1. In general, the morphologies of all samples consist of carbon spheres with a smooth surface.

The presence of 1.0 % of boron in the precursor solution induced a significant increase in the particle size, as well as an increase in the inhomogeneity of the size of the spheres.

TABLE I. Measured boron concentration and incorporation efficiency, and calculated Raman spectra parameters for the HTCB samples

Sample	c_B wt. %	B incorporation efficiency, %	Peak	Peak position cm^{-1}	Bandwidth cm^{-1}	I_D/I_G
HTCB ₀	–	–	D	1390	221	1.7
			G	1608	136	
HTCB _{0.2}	0.12	60	D	1389	218	1.7
			G	1605	130	
HTCB _{0.6}	0.38	63	D	1382	220	1.6
			G	1597	133	
HTCB ₁	0.72	72	D	1389	221	1.6
			G	1607	138	

As was previously shown,²⁹ more acidic conditions of starting glucose solutions induced by the addition of the boric acid could cause an enhancement of the hydrothermal reactions, which could induce particle condensation. The same trend of increasing particle size with the nominal concentration of boron is maintained after high temperature treatment.²²

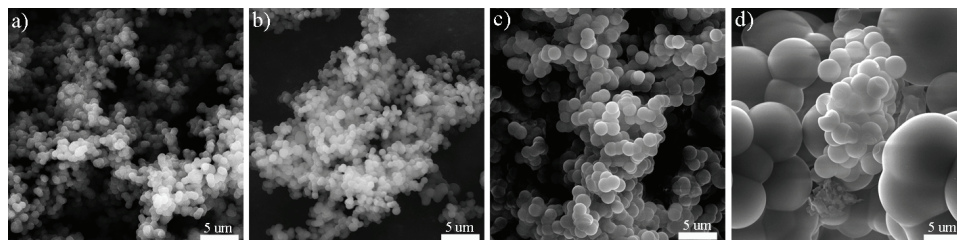


Fig. 1. SEM photographs of a) HTCB₀, b) HTCB_{0.2}, c) HTCB_{0.6} and d) HTCB₁.

The structural characteristics of the HTCB samples were analyzed by Raman spectroscopy. From the Raman spectra of the HTCB samples (Fig. 2), it could be noticed that the D and G peaks, which are characteristic of the disordered carbon structure, are very well defined.^{20,30,31} As previously shown,²² incorporation of boron into the structure of CHTCB samples to a nominal concentration of 0.6 wt. % induced some kind of structural ordering, but for the sample with a nominal boron concentration of 1.0 wt. %, deterioration of structural parameters was observed as a result of the greater lattice point occupation by boron atoms. Nevertheless, the peaks of the HTCB Raman spectra are similar to each other and significantly wide, which indicates a more disordered structure of the HTCB samples compared to the CHTCB samples. In order to analyze changes in the bonding

structure, Raman spectra parameters (peaks position, bandwidth and intensity, I_D and I_G) were obtained by deconvolution of the spectra (not shown here), using Gaussian fitting. Values of I_D/I_G (Table I) also confirm the higher degree of disorder for the HTCB samples compared to CHTCB. Namely, for CHTCB samples, the values of I_D/I_G were in the range from 0.9 to 1.2, while for HTCB samples the values were 1.6 or 1.7 and this difference is a direct consequence of the thermal treatment up to 1000 °C, which involves the formation of a more carbonic structure with a higher degree of structural arrangement.^{32–34} According to the Raman spectra parameters, B incorporation does not affect the structural characteristics of the HTCB samples.

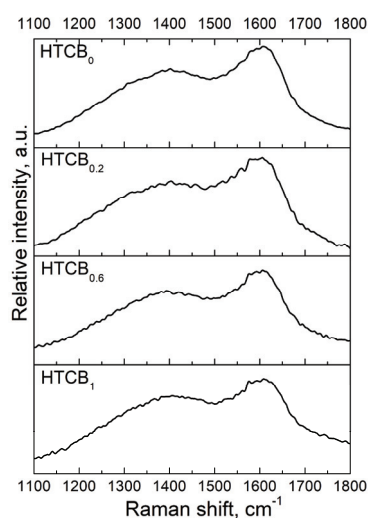


Fig. 2. Raman spectra of the HTCB samples.

Nitrogen adsorption-desorption isotherms for the HTCB samples, as the amount of N_2 adsorbed as function of relative pressure at -196 °C, are shown in Fig. 3.

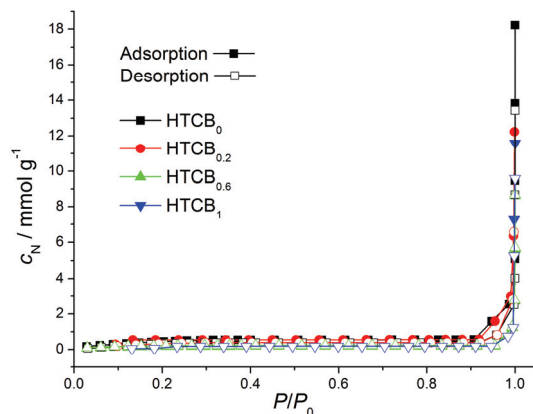


Fig 3. Nitrogen adsorption–desorption isotherms obtained for the HTCB samples.

According to the IUPAC classification,³⁵ the isotherms of the samples are of type II. Reversible type II isotherms are correlated with nonporous or macroporous adsorbents. The shape of isotherms is a consequence of the multilayer adsorption where thickness of the adsorbed multilayer sharply increases without limit at relative pressures close to 1. Specific surface areas calculated by the BET equation, S_{BET} , volume of micropores, V_{micro} , and mesoporous surface area, S_{meso} , are listed in Table II.

TABLE II. Textural characteristics of HTCB samples

Sample	$S_{\text{BET}} / \text{m}^2 \text{g}^{-1}$	$S_{\text{meso}} / \text{m}^2 \text{g}^{-1}$	$V_{\text{micro}} / 10^{-3} \text{cm}^3 \text{g}^{-1}$
HTCB ₀	9.87	6.24	0.54
HTCB _{0.2}	8.12	4.98	0.47
HTCB _{0.6}	4.03	2.19	0.35
HTCB ₁	4.98	2.93	0.39

The obtained S_{BET} values lie within 4–10 $\text{m}^2 \text{g}^{-1}$ for all the tested samples and, along with other presented textural characteristics, confirm that the HTCB samples are nonporous. The reason for this lay in the chemical processes that follow hydrothermal carbonization, and involve carbonization and solubilization of the organics. Through these processes, tarry substances are formed, leading to plugging of the pores and cause the formation of carbon materials with closed porosity and very small values of the BET surface area.^{36–38}

The ΔS_{BET} values, which represent the magnitude of the change in the S_{BET} values after thermal treatment of HTCB samples, are shown in Fig. 4 ($\Delta S_{\text{BET}} = S_{\text{BET}}(\text{CHTCB}_x) - S_{\text{BET}}(\text{HTCB}_x)$). A significant difference in the S_{BET} values before and after HTT, of almost 40 times, can be noticed for the undoped sample (0.0 wt.% B). However, for B-doped samples, the differences in the S_{BET} values decrease drastically, without showing a strictly doping-level dependence, even having a negative value for the sample with the highest nominal boron concen-

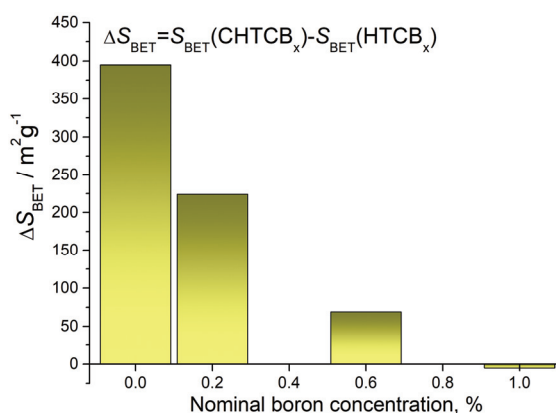


Fig. 4. The differences in S_{BET} values induced by subsequent carbonization of the HTCB samples.

tration (1.0 wt.% B). Based on this comparative analysis, it seems that the thermal treatment of undoped sample, HTCB₀, has an improvement effect on the surface area and porosity. On the contrary, the presence of B in the HTCB samples induced an inhibition of the development of the surface area for the final CHTCB samples. This may be a consequence of the alterations in the chemical reactions and processes, which follow the arranging carbon structure during carbonization, along with boron atom diffusion and its packing into the pores.^{22,39}

Hydrothermally derived carbons are generally characterized with abundant functional groups on their surface.⁴⁰ To analyze the type of surface oxygen groups, FT-IR analysis of HTCB samples was performed, and FT-IR spectra are shown in Fig. 5. The broad band between 3000 and 3700 cm⁻¹ is assigned to the stretching vibrations of O–H (hydroxyl or carboxyl), and the bands around 2815 to 3000 cm⁻¹ are the characteristic stretching vibrations of aliphatic C–H. The bands near 1706 cm⁻¹ and at 1622 cm⁻¹ are attributed to C=O and C–C vibrations, suggesting aromatization of the samples during the hydrothermal treatment.^{41,42} The peak at 1384 cm⁻¹ is related to the deformation vibration of the C–O bond in the carboxyl group,²² while the peaks in the range of 1300–1000 cm⁻¹ may originate from the stretching vibrations of the C–OH bond, or bending vibrations of the O–H bond, indicating the presence of hydroxyl groups.²² The peak at 797 cm⁻¹ originates from the out-of-plane bending vibration of the aromatic C–H bond, while the peak at 1510 cm⁻¹ originates from stretching vibrations of the aromatic ring.⁴³ It could be noted that the intensity of FT-IR spectra bands decreases for samples with higher boron content. A similar phenomenon was previously observed for carbonized HTCB samples.²² The reduction of the content of surface oxygen groups related to the presence of B atoms in carbon structure is a well-known phenomenon. One of the explanations for this phenomenon is the redistribution of charge in a carbon material, which occurs when boron is substituted into its structure in a way to block the otherwise accessible active sites, and protect them from interaction with oxygen.^{20,44}

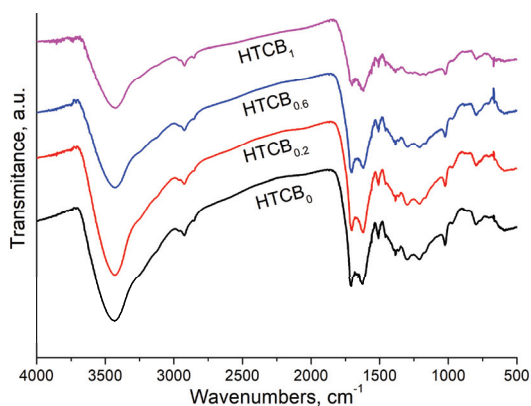


Fig. 5. FT-IR spectra of the HTCB samples.

The Boehm method was used to determine the acid/basic character of the HTC_B samples, through the amounts of acidic surface oxygen groups (carboxyl, lactone, phenol), and basic functionalities (chromene, ketone, and pyrone groups, along with the delocalized π -electrons of graphene layers). The results obtained by Boehm titrations (Table III) confirmed the influence that the incorporated boron has on the content of surface oxygen groups, through the trend of decreasing the number of surface oxygen groups with increasing boron content. The obtained results showed that basic groups are dominant on the surface of both HTC_B and CHTC_B types of samples. The total amount of functional groups present on the surfaces of CHTC_B samples was drastically lower, compared with HTC_B samples, which is the consequence of the applied thermal treatment, which leads to the conversion of the more disorder (hydrothermal) carbon structure into a carbon structure with more prominent aromatic character and hydrophobic properties, characteristic for carbon materials obtained by carbonization.¹²

TABLE III. Amount of acidic and basic surface oxygen groups for the HTC_B and carbonized HTC_B samples

Sample	Amount of acidic groups, mmol g ⁻¹	Amount of basic groups, mmol g ⁻¹
HTC _{B0}	1.142	4.695
HTC _{B0.2}	1.153	4.502
HTC _{B0.6}	0.925	1.892
HTC _{B1}	0.896	1.388
CHTC _{B0}	0.162	0.187
CHTC _{B0.2}	0.038	0.066
CHTC _{B0.6}	0.031	0.056
CHTC _{B1}	0.030	0.058

CONCLUSIONS

Hydrothermal carbonization of glucose in the presence of boric acid led to a significant incorporation of boron atoms into the structure of hydrothermal carbon samples. However, under the high-temperature treatment, most of the boron atoms leave the material structure, due to the weak bonding established between boron atoms and hydrothermal carbon structure. Boron addition of 1.0 % in precursor solution induced significant enhancement of particles size, although high-temperature treatment led to a decrease of the particle size as a consequence of mass loss and shrinkage processes, which occur during the treatment. The number of surface oxygen groups was reduced by incorporation of boron, and further, even more reduced by additional high-temperature treatment. Raman analysis showed that the boron-doped hydrothermal carbon samples are characterized by a lower carbonic structure with a lower degree of structural arrangement without a clear dependence between parameters values and boron content in the structure. Due to the structural transition that occurs during high-temperature treatment, carbon-

ized boron-doped samples show much higher values of the specific surface area compared to the boron-doped hydrothermal carbon samples, but inversely proportional to the content of boron, the presence of which has a strong inhibitory effect on the development of porosity. Nevertheless, comparison of the results obtained for hydrothermal carbons in different stages of synthesis suggest that the presence of boron brings significant changes in the characteristics of the material, hence boron doping represent an effective method for tailoring the structure, morphology, and surface properties of hydrothermally synthesized carbons.

Acknowledgement. The research was funded by the Ministry of Education, Science and Technological Development of the Republic of Serbia (Contracts No. 451-03-9/2021-14/200135, 451-03-9/2021-14/200287 and 451-03-9/2021-14/200017).

ИЗВОД

УТИЦАЈ ДОПИРАЊА БОРОМ НА КАРАКТЕРИСТИКЕ ХИДРОТЕРМАЛНИХ КАРБОНА НА БАЗИ ГЛУКОЗЕ

АНА М. КАЛИЈАДИС¹, МАРИНА М. МАЛЕТИЋ², АНЂЕЛИКА З. БЈЕЛАЈАЦ^{2,3}, БИЉАНА М. БАБИЋ⁴, ТАМАРА З. МИНОВИЋ АРСИЋ¹ и МАРИЈА М. ВУКЧЕВИЋ⁵

¹Лабораторија за материјале, Институт за нуклеарне науке Винча-Институт и националној значаја, Универзитет у Београду, Мике Пејровића Аласа 12–14, 11000 Београд, ²Иновациони центар Технолошко–металуршкој факултету, Карнеијева 4, 11000 Београд, ³C2N – Centre for Nanoscience and Nanotechnology Universite Paris-Saclay, 10 boulevard Thomas Gobert, 91120 Palaiseau, France, ⁴Институт за физику-Институт и националној значаја, Универзитет у Београду, Предревница 118, 11080 Београд и ⁵Технолошко–металуршкој факултету, Универзитет у Београду, Карнеијева 4, 11000 Београд

У овом раду испитан је утицај инкорпорације бора на структурне и површинске карактеристике хидротермалних карбона (НТСВ), добијених хидротермалном карбонизацијом глукозе у присуству различитих концентрација борне киселине, као прекурсора бора. Извршена је површинска и структурна карактеризација материјала, а добијени резултати су упоређени са карактеристикама накнадно карбонизованих НТСВ. Резултати су показали да хидротермални карбон на бази глукозе нема развијену порозност, а присуство бора у структури ових материјала нема значајнијег утицаја на специфичну површину. С друге стране, додатна карбонизација повећава специфичну површину недопираног узорка, а повећање садржаја бора доводи до драстичног смањења специфичне површине. Допирање бором доводи до смањења количине површинских кисеоникових група, како код хидротермално синтетисаних, тако и код додатно карбонизованих материјала. Анализом Раманских спектра утврђено је да садржај бора не утиче на структурно уређење узорака НТСВ, као и да накнадна карбонизација доводи до повећања уређености структуре. Поређење структурних и површинских карактеристика хидротермалних карбона допираних бором и накнадно карбонизованих материјала допринеће разјашњењу утицаја инкорпорације бора на карактеристике ових материјала.

(Примљено 11. октобра 2021, ревидирано 30. децембра 2021, прихваћено 3. јануара 2022)

REFERENCES

1. M. W. Moon, H. Y. Kim, A. Wang, A. Vaziri, *J. Nanomater.* **2015** (2015) 916834 (<http://dx.doi.org/10.1155/2015/916834>)

2. A. Hirsch, The era of carbon allotropes, *Nat. Mater.* **9** (2010) 868 (<https://doi.org/10.1038/nmat2885>)
3. M. M. Titirici, M. Antonietti, *Chem. Soc. Rev.* **39** (2010) 103 (<https://doi.org/10.1039/b819318p>)
4. Y. Wang, L. Qiu, M. Zhu, G. Sun, T. Zhang, K Kang, *Sci. Rep.* **9** (2019) 5535 (<https://doi.org/10.1038/s41598-019-38849-4>)
5. P. Zhu, J. Liu, J. Ma, L. Li, X. Zhang, *J. Biobased. Mater. Bio.* **15** (2021) 97 (<https://doi.org/10.1166/jbmb.2021.2030>)
6. C. Falco, F. Perez Caballero, F. Babonneau, C. Gervais, G. Laurent, M. M. Titirici, N. Baccile, *Langmuir* **27** (2011) 14460 (<https://doi.org/10.1021/la202361p>)
7. M. M. Titirici, A. Thomas, M. Antonietti, *New J. Chem.* **31** (2007) 787 (<https://doi.org/10.1039/b616045j>)
8. X. Zhu, Y. Liu, F. Qian, S. Zhang, J. Chen, *Energy Fuels* **29** (2015) 5222 (<https://doi.org/10.1021/acs.energyfuels.5b00512>)
9. X. Sun, Y. Li, *Angew. Chem. Int. Ed.* **43** (2004) 597 (<https://doi.org/10.1002/anie.200352386>)
10. Y. Z. Jin, C. Gao, W. Kuang Hsu, Y. Zhu, A. Huczko, M. Bystrzejewski, M. Roe, C. Y. Lee, S. Acquah, H. Kroto, D. R. M. Walton, *Carbon* **43** (2005) 1944 (<https://doi.org/10.1016/j.carbon.2005.03.002>)
11. S. A. Nicolae, H. Au, P. Modugno, H. Luo, A. E. Szego, M. Qiao, L. Li, W. Yin, H. J. Heeres, N. Berge, M. M. Titirici, *Green Chem.* **22** (2020) 4747 (<https://doi.org/10.1039/d0gc00998a>)
12. A. Kalijadis, N. Gavrilov, B. Jokić, M. Gilić, A. Krstić, I. Pašti, B. Babić, *Mater. Chem. Phys.* **239** (2020) 122120 (<https://doi.org/10.1016/j.matchemphys.2019.122120>)
13. M. M. Titirici, R. J. White, C. Falco, M. Sevilla, *Energy Environ. Sci.* **5** (2012) 6796 (<https://doi.org/10.1039/c2ee21166a>)
14. Y. J. Lee, Y. Uchiyama, Lj. R. Radovic, *Carbon* **42** (2004) 2233 (<https://doi.org/10.1016/j.carbon.2004.04.030>)
15. X. Wu, Lj. R. Radovic, *Carbon* **43** (2005) 1768 (<https://doi.org/10.1016/j.carbon.2005.02.029>)
16. Y. J. Lee, H. J. Joo, Lj. R. Radovic, *Carbon* **41** (2003) 2591 ([https://doi.org/10.1016/S0008-6223\(03\)00372-5](https://doi.org/10.1016/S0008-6223(03)00372-5))
17. J. S. Đorđević, A. M. Kalijadis, K. R. Kumrić, Z. M. Jovanović, Z. V. Laušević, T. M. Trtić-Petrović, *Cent. Eur. J. Chem.* **10** (2012) 1271 (<https://doi.org/10.2478/s11532-012-0042-1>)
18. S. Marinkovic, in *Chemistry and physics of carbon*, P. A. Thrower, Ed., Marcel Dekker Inc., New York, 1984., p. 1
19. Z. Huang, X. Liu, K. Li, D. Li, Y. Luo, H. Li, W. Song, L. Q. Chen, Q. Meng, *Electrochem. Commun.* **9** (2007) 596 (<https://doi.org/10.1016/j.elecom.2006.10.028>)
20. A. Kalijadis, Z. Jovanović, M. Laušević, Z. Laušević, *Carbon* **49** (2011) 2671 (<https://doi.org/10.1016/j.carbon.2011.02.054>)
21. A. Kalijadis, Z. Jovanović, I. Cvijović-Alagić, Z. Laušević, *Nucl. Instrum. Methods, B* **316** (2013) 17 (<http://dx.doi.org/10.1016/j.nimb.2013.08.030>)
22. A. Kalijadis, J. Đorđević, T. Trtić-Petrović, M. Vukčević, M. Popović, V. Maksimović, Z. Rakočević, Z. Laušević, *Carbon* **95** (2015) 42 (<http://dx.doi.org/10.1016/j.carbon.2015.08.016>)
23. C. Falco, N. Baccile, M. M. Titirici, *Green Chem.* **13** (2011) 3273 (<http://dx.doi.org/10.1039/c1gc15742f>)

24. J. A. Libra, K. S. Ro, C. Kammann, A. Funke, N. D. Berge, Y. Neubauer, M. M. Titirici, C. Fühner, O. Bens, J. Kern, K. H. Emmerich, *Biofuels* **2** (2011) 89 (<http://dx.doi.org/10.4155/bfs.10.81>)
25. A. D. Roberts, X. Li, H. Zhang, *Chem. Soc. Rev.* **43** (2014) 4341 (<http://dx.doi.org/10.1039/c4cs00071d>)
26. P. Zhang, Z. A. Qiao, S. Dai, *Chem. Commun.* **51** (2015) 9246 (<http://dx.doi.org/10.1039/c5cc01759a>)
27. B. C. Lippens, B. G. Linsen, J. H. de Boer, *J. Catal.* **3** (1964) 32 ([https://doi.org/10.1016/0021-9517\(64\)90089-2](https://doi.org/10.1016/0021-9517(64)90089-2))
28. A. M. Kalijadis, M. M. Vukčević, Z. M. Jovanović, Z. V. Laušević, M. D. Laušević, *J. Serb. Chem. Soc.* **76** (2011) 757 (<http://dx.doi.org/10.2298/JSC091224056K>)
29. M. M. Titirici, in *Novel Carbon Adsorbents*, J. M. D. Tascón, Ed., Elsevier, Oxford, 2012, p. 351 (<http://dx.doi.org/10.1016/B978-0-08-097744-7.00012-0>)
30. A. C. Ferrari, J. Robertson, *Phys. Rev., B* **61** (2000) 14095 (<https://doi.org/10.1103/PhysRevB.61.14095>)
31. S. Urbonaitė, L. Halldahl, G. Svensson, *Carbon* **46** (2008) 1942 (<https://doi.org/10.1016/j.carbon.2008.08.004>)
32. Z. Wang, H. Ogata, G. J. Hong Melvin, M. Obata, S. Morimoto, J. Ortiz-Medina, R. Cruz-Silva, M. Fujishige, K. Takeuchi, H. Muramatsu, T. Y. Kim, Y. A. Kim, T. Hayashi, M. Terrones, Y. Hashimoto, M. Endo, *Carbon* **121** (2017) 423 (<http://dx.doi.org/10.1016/j.carbon.2017.06.003>)
33. H. Fujimoto, *Carbon* **41** (2003) 1585 ([http://dx.doi.org/10.1016/S0008-6223\(03\)00116-7](http://dx.doi.org/10.1016/S0008-6223(03)00116-7))
34. Z. Q. Li, C. J. Lu, Z. P. Xia, Y. Zhou, Z. Luo, *Carbon* **45** (2007) 1686 (<http://dx.doi.org/10.1016/j.carbon.2007.03.038>)
35. K. S. W. Sing, D. H. Everett, R. A. W. Haul, L. Moscou, R. A. Pierotti, J. Rouquerol, T. Siemieniowska, *Pure Appl. Chem.* **57** (1985) 603 (<https://doi.org/10.1351/pac198557040603>)
36. S. E. Elaigwu, G. M. Greenway, *Int. J. Ind. Chem.* **7** (2016) 449 (<http://dx.doi.org/10.1007/s40090-016-0081-0>)
37. M. M. Titirici, M. Antonietti, N. Baccile, *Green Chem.* **10** (2008) 1204 (<http://dx.doi.org/10.1039/b807009a>)
38. M. Sevilla, A. B. Fuertes, *Chem. Eur. J.* **15** (2009) 4195 (<http://dx.doi.org/10.1002/chem.200802097>)
39. S. Karthikeyan, K. Viswanathan, R. Boopathy, P. Maharaja, G. Sekaran, *J. Ind. Eng. Chem.* **21** (2015) 942 (<https://doi.org/10.1016/j.jiec.2014.04.036>)
40. S. Kubo, I. Tan, R. J. White, M. Antonietti, M. M. Titirici, *Chem. Mater.* **22** (2010) 6590 (<http://dx.doi.org/10.1021/cm102556h>)
41. Y. Gao, X. Wang, J. Wang, X. Li, J. Cheng, H. Yang, H. Chen, *Energy* **58** (2013) 376 (<http://dx.doi.org/10.1016/j.energy.2013.06.023>)
42. Z. Zhang, K. Wang, J. D. Atkinson, X. Yan, X. Li, M. J. Rood, Z. Yan, *J. Hazard. Mater.* **229–230** (2012) 183 (<http://dx.doi.org/10.1016/j.jhazmat.2012.05.094>)
43. M. Zbair, M. Bottlinger, K. Ainassaari, S. Ojala, O. Stein, R. L. Keiski, M. Bensitel, R. Brahmī, *Waste Biomass Valor.* **11** (2020) 1565 (<https://doi.org/10.1007/s12649-018-00554-0>)
44. Lj. R. Radovic, M. Karra, K. Skokova, P. A. Thrower, *Carbon* **36** (1998) 1841 ([https://doi.org/10.1016/S0008-6223\(98\)00156-0](https://doi.org/10.1016/S0008-6223(98)00156-0)).